Odorant Binding and Conformational Changes of a Rat Odorant-binding Protein

C. Nespoulous[1], L. Briand[1], M.-M. Delage[1], V. Tran[2,3] and J.-C. Pernollet[1]

[1]INRA, Biochimie et Structure des Protéines, 78352 Jouy-en-Josas, France and [2]INRA, Physico-Chimie des Macromolécules, 44316 Nantes, France
[3]Present address: Universite de Nantes & CNRS, Biocatalyse, 44322 Nantes, France

Correspondence to be sent to: C. Nespoulous, INRA, Biochimie et Structure des Protéines, 78352 Jouy-en-Josas, France. e-mail: nespoulo@jouy.inra.fr

Abstract

Odorant-binding proteins (OBPs) are lipocalins secreted in the nasal mucus of vertebrates, which convey odorants to their neuronal receptors. We compared the binding properties of a recombinant rat OBP (OBP-1F) using a set of six odorants of various chemical structures. We examined the binding properties by both fluorescent probe competition and isothermal titration calorimetry. OBP-1F affinity constants, in the micromolar range, varied by more than one order of magnitude and were roughly correlated to the odorant size. The observed binding stoichiometry was found to be around one odorant per dimer. Using tyrosine differential spectroscopy, the binding of ligand was shown to induce local conformational changes. A three-dimensional structure of OBP-1F, modelled using the known structure of aphrodisin as template, allowed us to suggest the location of the observed structural changes outside of the binding pocket. These results are consistent with one binding site located in one of the two β-barrels of the OBP-1F dimer and a subtle conformational change correlated with binding of an odorant molecule, which hampers uptake of a second odorant by the other hydrophobic pocket.

Key words: ligand–protein interaction, lipocalin, microcalorimetry, olfaction, UV spectroscopy

Introduction

In order to reach their membrane receptors embedded in the membrane of olfactory neurons, airborne odorants, which are commonly hydrophobic molecules, have to be conveyed through the aqueous nasal mucus. The odorant-binding proteins (OBPs), which are abundant low-mol. wt soluble proteins (~20 kDa) secreted by the olfactory epithelium in the nasal mucus of vertebrates, are candidates for playing such a carrier role (Steinbrecht, 1998). These proteins reversibly bind odorants with dissociation constants in the micromolar range. Although their functions are still unclear, OBPs are also suspected to participate in the deactivation of odorants (Pelosi, 1996; Lazar et al., 2002).

Vertebrate OBPs belong to the lipocalin superfamily (Flower et al., 2000; Tegoni et al., 2000). Although members of this family display low sequence similarity (usually <20% amino acid identity), all share a conserved folding pattern, an eight-stranded β-barrel flanked by an α-helix at the C-terminal end of the polypeptide chain. The β-barrel defines a central apolar cavity, called the calyx, whose role would be to bind and transport hydrophobic odorant molecules (Bianchet et al., 1996; Tegoni et al., 1996; Spinelli et al.,

1998). Several OBPs have been shown to be present as dimers, but others seem to exist as monomeric species (Pelosi, 1994). Nevertheless, in some cases, such as porcine OBP-1, the oligomeric state remains questionable because controversial results, provided by different methods, have been reported (Spinelli et al., 1998; Burova et al., 1999).

OBPs have been identified in a variety of species, including cow, pig, rabbit, mouse, rat and, recently, elephant and human (Pevsner et al., 1985, 1988; Dal Monte et al., 1991; Pes et al., 1992; Pes and Pelosi, 1995; Briand et al., 2000b, 2002; Lazar et al., 2002). Since the discovery of the first vertebrate OBP isolated from the bovine nasal mucus (Pelosi et al., 1982; Bignetti et al., 1985), different OBP subtypes have been reported to occur simultaneously in the same animal species. Three have been described in pig (Dal Monte et al., 1991; Scaloni et al., 2001), four in mouse (Miyawaki et al., 1994; Pes et al., 1998; Utsumi et al., 1999), three in rat (Pevsner et al., 1988; Dear et al., 1991a, 1991b; Ohno et al., 1996; Briand et al., 2000b; Löbel et al., 2001), three in rabbit (Garibotti et al., 1997) and at least eight in porcupine (Felicioli et al., 1993; Ganni et al., 1997).

Rat OBP binding properties have been investigated by spectroscopic approaches using fluorescent probe competitive assays and by isothermal titration calorimetry, demonstrating that the three OBPs are specially tuned towards distinct chemical classes of odorants. Rat OBP-1 preferentially binds heterocyclic compounds such as pyrazine derivatives (Löbel *et al.*, 1998; Briand *et al.*, 2000b). OBP-2 appears to be more specific for long-chain aliphatic aldehydes and carboxylic acids (Löbel *et al.*, 1998), whereas OBP-3 was described to interact strongly with odorants composed of saturated or unsaturated ring structure (Löbel *et al.*, 2001).

Here we examined the binding properties of the rat variant OBP-1F, originating from the Fisher rat strain, for several odorants comparing both fluorescent probe competition and isothermal titration calorimetry. In addition to IBMP, a model odorant systematically used in OBP studies, the tested odorants were chosen among molecules largely used in the food industry, exhibiting different odors and persistence and belonging to different chemical classes. We also investigated the conformational changes of the protein upon ligand binding and their possible implications on the binding stoichiometry of the dimeric protein.

Materials and methods

Protein purification

Recombinant rat OBP-1F was produced using the yeast *Pichia pastoris* according to Briand *et al.* (2000b), but purified by reversed phase liquid chromatography (RPLC) performed using an Aquapore C8 column (Prep –10, 1.0 i.d. × 3.0 cm; Perkin Elmer, France). After filtration aimed to remove insoluble components from *P. pastoris* supernatant containing recombinant protein, the solution was dialysed for 4 days at 4°C, using a dialysis tube with 12 000 Da cut off (Servapor, Polylabo, France) and lyophilized. The lyophilized supernatant was resuspended in eluent A (25 mM ammonium acetate, pH 7.0, 5% V/V acetonitrile in H_2O) and the column was equilibrated with the same eluent. After sample loading, the column was extensively washed with eluent A. Elution was run using a linear gradient to 30% eluent B (25 mM ammonium acetate, pH 7.0, 60% V/V acetonitrile in H_2O) in the first 10 min with a 10 min hold gradient. OBP-1F elution was then achieved using a linear gradient to 70% eluent B in 40 min. The flow rate was 2 ml/min and the absorbance was recorded at 275 nm. The fractions containing OBP-1F eluted around 35% CH_3CN were pooled, dialysed extensively against MilliQ H_2O and lyophilized. Several batches of protein were produced and randomly used for repeated experiments.

Extraction of endogenous OBP-1F ligand

Approximately 750 μg of lyophilized OBP-1F were dissolved in 50 μl of 25 mM ammonium acetate buffer, pH 8.0. OBP-1F was then extracted using 50 μl of $CHCl_3$ with vigorous vortexing at room temperature. After centrifugation at 10 000 × g for 30 min at 4°C, the $CHCl_3$ extract was analysed by gas chromatography (GC) using a GC 8000 Series 8180 Fisons Instrument (Thermoquest) as already reported in Briand *et al.* (2000b). An aliquot of ammonium acetate buffer (50 μl) was treated with the same extraction procedure and used as a control.

Odorants

The molecules used, hydroxy-butanone [(±)-3-hydroxy-butan-2-one], ethyl-butyrate [ethyl-*n*-butanoate], γ-deca-lactone [(±)-γ-*n*-hexyl-γ-butyrolactone], eugenol [4-allyl-2-methoxyphenol] and linalool [(±)-3,7-dimethyl-1,6-octadien-3-ol], were generous gifts of SKW Biosystems (Grasse, France). IBMP [2-iso-butyl-3-methoxypyrazine], an odorant used as a standard in OBP studies, was purchased from Acros Organics.

Fluorescence-based ligand binding

The fluorescent probe 1-aminoanthracene (1-AMA) was from Fluka. The competitive binding assays, aimed to displace the probe with ligands, were performed with 2 μM of OBP-1F in 50 mM potassium phosphate buffer, pH 7.5, with 2 μM 1-AMA concentration. OBP-1F concentration was determined using UV spectroscopy employing a extinction coefficient of 14 173/M/cm at 276.3 nm, measured according to Pace *et al.* (1995). The fluorescent probe and odorants were dissolved in 10% v/v MeOH as 1 mM stock solution. Successive 1 μl odorant solution aliquots were added to 1 ml of OBP-1F solution. Spectra were recorded at 25°C using a SFM 25 Kontron fluorometer with a 5 nm bandwidth for both excitation and emission. No cut off filter was used in the excitation beam. The excitation wavelength used for 1-AMA was 290 nm. Once the binding equilibrium has been reached, in ~1 min as verified by time course experiments (not shown), the relative proportion of probe bound to OBP-1F was calculated by measuring fluorescence emission (expressed in arbitrary units) recorded at 485 nm. Competitor concentrations causing fluorescence decay to half-maximal intensity were taken as IC_{50} values. The dissociation constant K_d values were calculated as $K_d = [IC_{50}]/(1 + [AMA]/K_d^{AMA})$ with [AMA] being the fluorophore concentration and K_d^{AMA} (0.6 μM) the OBP-1F-AMA complex dissociation constant (Briand *et al.*, 2000b; Ramoni *et al.*, 2001). A reverse experiment was carried out in which linalool, used as a first ligand, was displaced by 1-AMA, used as a competitor. The similar method as described above was used to calculate the apparent K_d of linalool.

Isothermal titration calorimetry

Isothermal titration calorimetry (ITC) experiments were carried out at 30°C with an MCS System (MicroCal) microcalorimeter as previously described (Briand *et al.*, 2001). OBP-1F concentration (20–30 μM in 50 mM phosphate

buffer, pH 7.0 in the cell, 1.34 ml) was determined as above. Protein samples were sterile filtered before degassing. Ligand solutions were injected in 40 successive 5 μl aliquots at 4 min interval. MeOH content in the ligand solution never exceeded 0.5%. Raw data were processed with Microcal Origin software and the variation of enthalpy was fitted by using different models of several binding sites per dimer. Binding data, i.e. the number of binding sites (n), the binding constant (K_a) and the binding enthalpy (ΔH_b), were determined as parameters of the calculated curves best ajusted to the experimental binding isotherms by the nonlinear least-squares minimization method (Fisher and Singh, 1995).

Circular dichroism

Circular dichroism (CD) spectra were recorded using a Jasco J-810 spectropolarimeter and analysed as previously described (Briand et al., 2000b). OBP-1F concentration (~0.5–1 mg/ml in phosphate buffer) was determined using UV spectroscopy as described above. Protein solutions were placed in a 1 cm path-length cell. Baseline was recorded with the same buffer with or without ligand and was subtracted from the protein spectrum.

UV difference spectroscopy

Spectrophotometric titration of tyrosines were performed as reported by Nespoulous and Pernollet (1994). Difference spectra were directly measured on a double beam Perkin-Elmer Lambda 6 spectrophotometer. Protein solutions (~3.5 mg/ml in 50 mM phosphate buffer, pH 7.0, determined using UV spectroscopy as described above) were placed in quartz cells (path-length 10 mm). Difference spectra were performed between the reference OBP solution at neutral pH and the sample solution in which microliters of NaOH dilutions in water were directly added to the cell to increase pH. The same volumes of water were added to the reference cell to make the same dilution. The pH in the magnetic stirred cell was controlled using a glass electrode. The number of ionized tyrosyl residues was calculated using the difference absorption measured at 295 nm and the molar absorption change of 2330/M/cm for one tyrosyl residue. All spectra were recorded at room temperature.

Molecular modelling

Sequence analysis and pairwise alignments were performed using the BLAST2 and ClustalW algorithms on the PBIL (http://pbil.univ-lyon1.fr) web site. Sequence alignment was optimized on the basis of secondary structure conservation of the selected lipocalin structure: equine Equ c 1 [PDB code 1EW3 (Lascombe et al., 2000)] and bovine Bos d 2 [PDB code 1BJ7 (Rouvinen et al., 1999)] allergens, mouse major urinary protein [PDB code 1MUP (Bocskei et al., 1992)], porcine OBP [PDB code 1A3Y (Spinelli et al., 1998)] and hamster aphrodisin [PDB code 1E5P (Vincent et al., 2001)]. Three-dimensional models were builded with MODELLER (Accelrys) software (Sali and Blundell, 1993)

using all the selected crystallographic structures. Energy of structures and geometrical parameters were minimized using Charmm (Brooks et al., 1988) and models were assessed using PROCHECK (Laskowski et al., 1993).

Results

Odorant-binding properties

In order to improve the removal of potentially bound hydrophobic ligands, we purified OBP-1F using one-step RPLC in place of the previous reported protocol (Briand et al., 2000b). The activity of samples from both purification protocols was measured using the methods described below and revealed no significant difference.

A fluorescence assay was employed for binding experiments using 1-AMA as a probe in addition to ITC, a direct physical method, for assessing ligand–protein interactions. When excited at 290 nm, 1-AMA presented a weak fluorescence emission with a maximum at 515 nm in aqueous medium. In the presence of OBP-1F, the emission maximum underwent a hypsochrome shift towards 485 nm, with a 15-fold quantum yield increase. Titration of OBP-1F with 1-AMA was saturable ($K_d^{AMA} = 0.6 \pm 0.3$ μM) as already observed (Briand et al., 2000b), showing that OBP-1F activity was conserved after RPLC purification. Six odorants (Fig. 1A), IBMP, eugenol, linalool, γ-decalactone, ethyl-butyrate and hydroxy-butanone, were used with different ability to displace the fluorescent probe. Figure 1B illustrates the competition curves obtained with these odorants at pH 7.5. We verified that the reaction equilibrium was reached before data collection and used MeOH in order to dissolve ligands and probes, because this solvent is known not to compete with 1-AMA (Briand et al., 2000b). The added quantity of MeOH, which did not exceed 0.1% v/v (final concentration) did not obviously decrease the polarity of the medium, as observed in control experiments run with the probe only, in the absence of protein (not shown). The fluorescence intensity of OBP-1F-probe complexes was severely reduced with eugenol, IBMP, γ-decalactone and linalool, while the effects of ethyl-butyrate and hydroxy-butanone could be considered as weak. The calculated apparent dissociation constants (K_d), deduced from the half-maximal values (IC_{50}), were less than the micromolar range for the four most active odorants and two orders of magnitude higher for the less active ones (Table 1).

Binding experiments with the same odorants were further conducted using ITC. Titration calorimetric curves obtained with eugenol at pH 7.0 (Fig. 2) clearly showed that eugenol binding was saturable with about one apparent site per dimer, as indicated by the abscissa of the inflection point as already reported for porcine OBP using the same method (Burova et al., 1999). With the exception of hydroxy-butanone, which proved unable to bind OBP-1F by this approach, all other tested molecules exhibited a binding isotherm at neutral pH. Binding constants and thermo-

dynamic parameters for the five bound odorants are presented in Table 1. The binding stoichiometry for the odorant–OBP-1F interaction did not reach one site per dimer, except for IBMP. It can be explained by the presence of partially inactive proteins as already reported (Löbel *et*
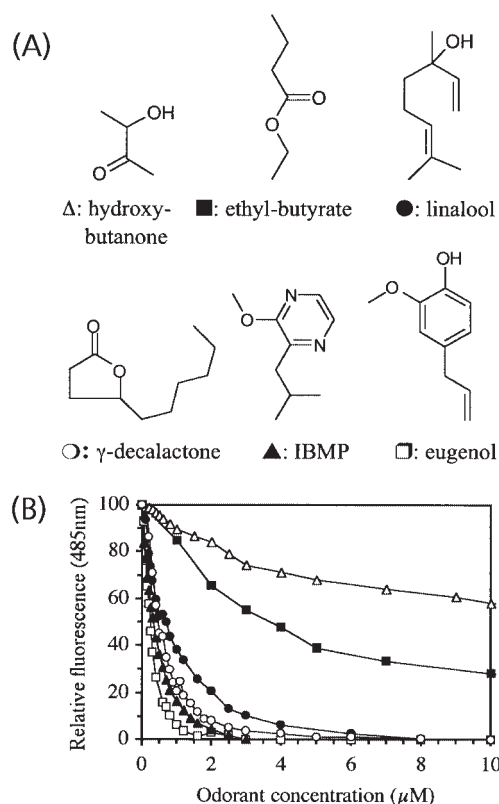
al., 2001). The occupation of binding sites by lipophilic ligands tightly bound onto OBP, not removed during the purification process, has been already observed (Marchese *et al.*, 1998; Burova *et al.*, 2000; Ramoni *et al.*, 2001; Oldham *et al.*, 2001). Volatile compounds potentially bound to OBP-1F were extracted with $CHCl_3$ and analyzed by GC, which did not reveal any component associated with the protein (data not shown). However, the presence of more polar compounds not extracted by $CHCl_3$ or not sufficiently volatile to be analyzed by GC, cannot totally be excluded.

In Table 1, the association constants obtained with ITC are compared to those obtained by competition fluorescence assay. Fluorescence measurements revealed greater apparent affinity for all ligands tested than ITC. The discrepancy in the magnitude of values between both measurements was likely due to the complexity of the indirect measurement of the fluorescence assay, in contrast with the results obtained with rat OBP-3 for binding of two odorants (Löbel *et al.*, 2001). There are thus three possible reasons for the discrepancy: (i) the occurrence of multiple competing equilibria; (ii) the presence of allosteric effects across the dimer; or (iii) different binding kinetics associated with protein conformational changes during 1-AMA displacement. When a reverse experiment was carried out using 1-AMA as a ligand to displace linalool from OBP-1F, we obtained an apparent K_d value with the same calculation method, which was 10 times higher than that measured when linalool displaced 1-AMA. Such a discrepancy might reveal either a complex mechanism in which all ligands are not similarly bound, implying that displacement cannot be equivalent to competition, or the weakness of the calculation of K_d from IC_{50}. Fluorescence competitive assays using IC_{50} therefore provides only apparent constants, only useful to classify ligands tested in the same experimental conditions.

When comparing data originating from ITC obtained at pH 7.0, eugenol, IBMP and linalool exhibited very close affinity for OBP-1F in the micromolar range, whereas γ-decalactone and ethyl-butyrate showed affinity, respec-

Figure 1 **(A)** Chemical structure of the odorants used in binding experiments. **(B)** 1-AMA fluorescence competitive binding assay. Fluorescence emission spectra were recorded at 25°C with 2 μM 1-AMA in presence of 2 μM recombinant OBP-1F; excitation and emission wavelengths were 290 and 485 nm, respectively. Odorants used: hydroxy-butanone (open triangles), ethyl-butyrate (filled squares), linalool (filled circles), γ-decalactone (open circles), 2-isobutyl-3-methoxypyrazine (IBMP; filled triangles) and eugenol (open squares); fluorescence of probe-protein complexes were assigned to 100% in absence of competitor.

Table 1 Thermodynamic parameters of odorant binding to OBP-1F dimer at 30°C obtained by ITC and affinity constants determined through fluorescence competitive assays

Odorants (mol. wt)	ΔH_b (kJ/mol)	ΔS_b (J/mol)	ΔG_b (kJ/mol)	n (number of sites)	K_a^{ITC} $(10^{-6}/M)^a$	$1/K_d^{fluo}$ $(10^{-6}/M)^b$
Hydroxy-butanone (88)	–	–	–	–	–	0.096
Ethyl-butyrate (116)	−34.1 ± 1.4	−2.3	−33.5	0.7 ± 0.02	0.58 ± 0.11	0.29
γ-Decalactone (170)	−64.8 ± 0.7	−98.0	−35.1	0.8 ± 0.01	1.10 ± 0.08	9.63
Linalool (154)	−42.7 ± 0.8	−19.6	−36.7	0.6 ± 0.01	2.14 ± 0.33	6.67
IBMP (166)	−35.3 ± 0.9	4.2	−36.6	1.1 ± 0.02	2.32 ± 0.57	14.44
Eugenol (164)	−63.1 ± 1.1	−86.4	−36.9	0.7 ± 0.01	2.41 ± 0.33	21.67

[a]K_a^{ITC}: association constant determined by ITC experiments.
[b]K_d^{fluo}: dissociation constant determined by fluorescent experiments.
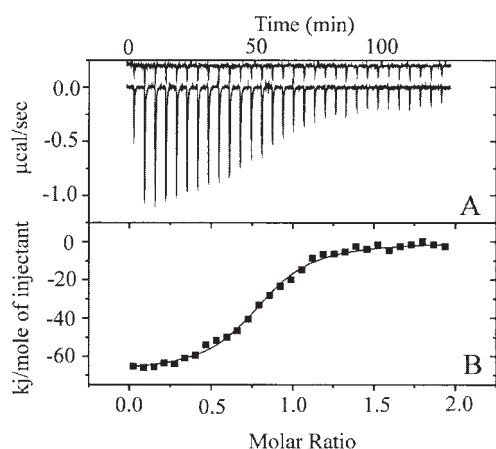Dashes indicate impossibility of measurements.

Figure 2 Isothermal titration calorimetry curves of eugenol binding to OBP-1F. **(A)** Raw data of representative ITC experiments; upper curve, control with buffer in the cell and odorant in the syringe; lower curve, protein solution in the cell and odorant in the syringe. **(B)** Binding enthalpies corrected for heat of ligand dilution. Solid line, curve fitting obtained by a model of one site per dimer. Protein concentration, 22 μM in phosphate buffer pH 7.0. Controlled temperature, 30°C.

tively two and four times lower than that of eugenol. Binding of hydroxy-butanone was very weak and measurable only by fluorescence assay. The Gibbs free energy of each interaction was similar, but differences in the variations of enthalpy and entropy indicate that binding of these structurally different odorants involved specific constraints and interactions at the molecular level in the binding site.

Conformational changes upon ligand binding

Binding assays reported above allowed us to select two odorants for their representative affinity toward OBP-1F, hydroxy-butanone and linalool, with low and high affinity, respectively, in order to perform structural studies. Ligand-binding induced conformational changes generally modify the protein spectral properties, which can be followed by UV spectroscopy. Because of the large protein amounts needed for such experiments, spectroscopy measurements were carried out only with the two selected ligands.

The pH spectrophotometric titration allowed the measurement of tyrosine pK, whose variation clearly showed a local structural change. The OBP-1F titration curve was shifted to alkaline pH in the presence of odorant (Fig. 3). All titration curves presented the same two-steps shape and only five tyrosines among six were titrated at pH 13. In the presence of hydroxy-butanone and methanol, the shift was only very limited. In the presence of linalool, the basic shift was ~0.5 pH unit for the second inflexion point from 11.5 to 12. Analysis of the titration data according to Tachibana and Murachi (1966) showed that two tyrosyl residues were titrated with an apparent pK of 9.6 ± 0.03, close to that of the model compound N-acetyl-L-tyrosine ethyl ester (not shown), which corresponds to the first step of the titration curve until pH 11. Two other tyrosines were titrated with a
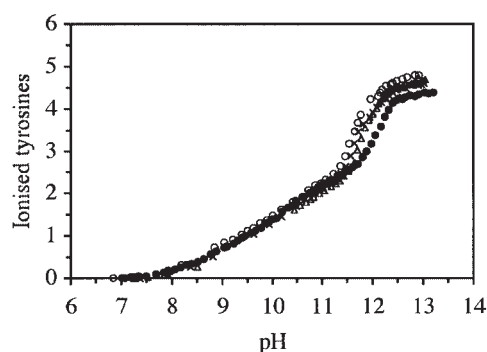

Figure 3 Spectrophotometric titration curves of tyrosyl residues of OBP-1F in absence (open circles) or in presence of ligands: linalool (filled circles), hydroxy-butanone (open triangles) and methanol (×). Protein concentration, 38 μM in phosphate buffer. Light path, 10 mm. Difference absorbance measured at 295 nm. ε for one tyrosyl residue at 295 nm: 2330/M/cm.
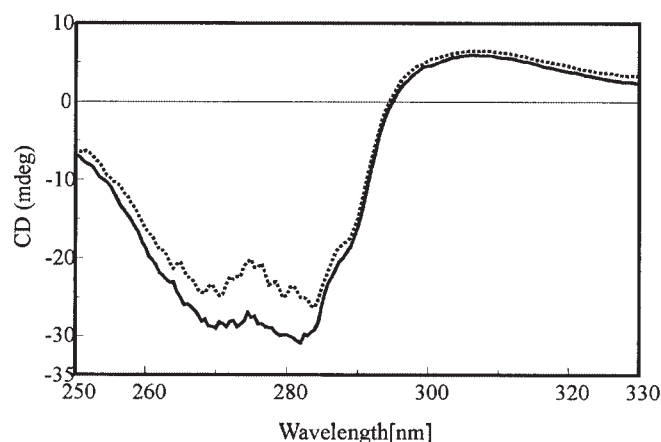

Figure 4 CD near UV spectra of OBP-1F in absence (solid line) or presence (dotted line) of linalool. Protein and linalool concentrations, 160 and 400 μM in phosphate buffer pH 7, respectively. Light path, 10 mm.

pK of 11.2 ± 0.06 corresponding to the second step of the curve. An intermediate tyrosyl residue was titrated between the above mentioned clusters, around pH 10.2 ± 0.03. In the presence of odorants, only the cluster of tyrosyl residues with a pK of 11.2 underwent a pK shift. In the case of linalool, it was shifted toward 11.7 ± 0.02.

The numbers of tyrosines involved in the binding and the induced modification were high enough to observe, through CD, a change in their environment. In the aromatic region, the CD spectrum was composed of two close negative peaks banding at 275 and 282 nm, attributed to tyrosine and both tyrosine and tryptophan side-chains, respectively, and a weak shoulder at 290 nm, attributed to a tryptophan side-chain. This indicates a highly asymmetric environment for the aromatic residues in the folded structure of OBP-1F (Fig. 4). In the presence of linalool, significant difference was observed for the 275 and 282 nm bands, whereas the shoulder at 290 nm seemed to be less slightly affected, likely

due to the general modification of the spectrum shape. This suggests a local conformational transition upon binding, leading to a flexible side-chain packing. No difference was observed in presence of hydroxy-butanone or methanol (not shown). The contribution to CD of linalool as a chiral compound proved to be negligible due to the absence of chemical group able to absorb light in the same UV region.

Molecular modelling

Among the members of the lipocalin superfamily whose 3D structure is known, five proteins (equine and bovine allergens, mouse major urinary protein, porcine OBP-I and hamster aphrodisin) were selected for their sequence identity with OBP-1F of >30%. A defined conserved core of secondary structure around the β-barrel allowed us to optimize the sequence alignment. At this initial stage of the homology molecular modelling, all these constructions have the same general shape because of the similarity between the initial templates (belonging to the retinol-binding, protein-like structural family). No further energy refinements would be able to segregate these models. Furthermore, the tyrosine positions and orientations are almost comparable in all our models. The model derived from aphrodisin using 1E5P.pdb coordinates (Vincent *et al.*, 2001) was finally selected for its higher sequence homology and the presence of four conserved cysteines. When superimposed with its template, the backbone trace of the OBP-1F model displayed a 1.04 Å root mean square deviation on 138 Cα atoms. The Ramachandran plot indicated that all residues present φ and ψ angles in the core and allowed regions and most bond lengths and angles were in the range of expected values.

Among the six OBP-1F tyrosines, three (Y38, Y78 and Y82) are highly conserved or replaced by a phenylalanine in the other lipocalins and one (Y20), which is less conserved (Fig. 5A). Except Y139, present at the C-terminal of the α-helix, all tyrosines are located in or close to a β-strand, around the β-barrel. No tyrosyl side-chains are oriented within the binding pocket shaped within the β-barrel structure except Y82, which is present at its opening. Two tyrosines (Y82 and Y87) display their hydroxyl group free to the solvent, whereas the other four are involved in one (Y20, Y78 and Y139) or two (Y38) H-bonds with neighbouring residues as shown in to Table 2 (Fig. 5B,C). The single tryptophan (W16) is located at the opposite side of the opening and outside of the binding site.

Discussion

Odorants of diverse structures and odors were comparatively tested using two different methods, a competition fluorescent assay, which is a complex mechanism involving a tripartite interaction, and, on the other hand, ITC, a direct physical measurement. Except for linalool and ethyl-butyrate, fluorescence measurements showed apparent affinities slightly different than ITC, depending on odorants, but revealed roughly the same order of affinity for OBP-1F.

Hydroxy-butanone, the smallest tested molecule (88.1 Da), was the only tested odorant observed by ITC not to bind OBP-1F, although able to very lightly displace 1-AMA fluorescence. It is likely that interactions between the atoms or atomic groups of the ligand and those of the amino acid side-chains of the binding pocket were not numerous enough to establish a stable binding and a strong affinity. It is more a matter of quantity than quality as already suggested for ligand binding on porcine OBP (Vincent *et al.*, 2000). Except for ethyl-butyrate, which binds OBP-1F slightly less strongly, ITC showed that the four tested ligands exhibited variable affinity in the micromolar range, as already published for other mammalian OBPs (Pelosi, 1994; Tegoni *et al.*, 2000). Odorant affinities can roughly be correlated to their molar masses, with the exception of γ-decalactone, whose affinity is smaller than those of other odorants of similar size (between 150 and 170 Da), likely due to the molecule shape, which is constituted of a heterocycle and a long alkyl tail. These results agree with a previous report, which described that the length and the size appeared to be a major selective criterion for recognition among the structural features of odorants involved in OBP binding (Pevsner *et al.*, 1990).

Binding free energies (Table 1) were found to be close to each others for all tested ligands and in the same range as those reported for other OBPs (Burova *et al.*, 1999; Löbel *et al.*, 2001). However, the balance between enthalpy and entropy variations differed from one odorant to another. In all cases, binding was favoured by enthalpy, but with some deviation, since ΔH was observed to be twice as high with eugenol than IBMP, for instance. Unlike enthalpy, the net entropy exchange varied by two orders of magnitude from ethyl-butyrate to γ-decalactone and even became positive with IBMP. Entropy driven IBMP binding partially balanced a weak net exchange in enthalpy. The variability of binding thermodynamic parameters, corresponding to structurally different ligands, suggests that particular constraints and different interactions occur within the binding site, as already mentioned for porcine OBP-1 (Vincent *et al.*, 2000).

Using UV spectroscopic methods, we show that OBP-1F undergoes a conformational change upon odorant binding. The observed measurement variations were shown to depend on ligand affinity and originated likely from the perturbation of the same residues. The spectral properties of aromatic residues depend on their immediate environment. It can vary due to the proximity of an external compound, with or without the side-chain moving, as reported in other lipocalins to occur between the conserved Y82 and some ligands (Vincent *et al.*, 2000; Spinelli *et al.*, 2002). A side-chain shift can also be induced by a distance conformational change of the protein backbone. However, the question of which residues are involved in this process remains. The CD spectrum change could be addressed to all the aromatic residues including the single tryptophan W16 of OBP-1F. But
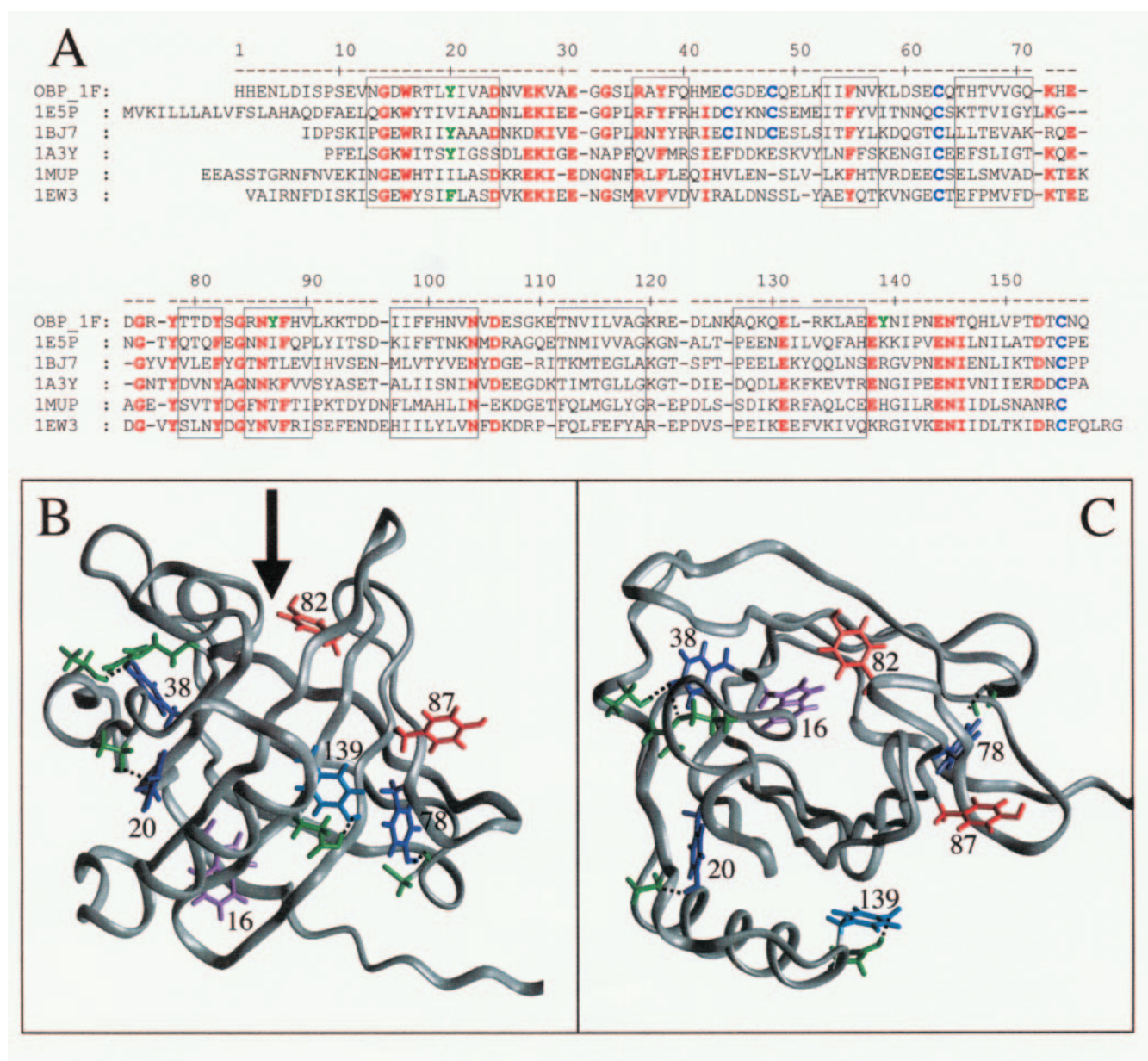
Figure 5 Molecular modelling of OBP-1F. **(A)** Sequences alignment of OBP-1F with lipocalins having a known 3D structure and a sequence homology over 30% with OBP-1F. Conserved residues are in red, cysteines are in blue and tyrosines less or not conserved in OBP-1F are in green. Boxes indicate conserved secondary structures. The PDB codes are: 1E5P, hamster aphrodisin; 1BJ7, bovine lipocalin allergen Bos d 2; 1A3Y, porcine OBP-I; 1MUP, mouse major urinary protein; 1EW3, equine lipocalin allergen Equ c 1. **(B, C)** Lateral and front views (with a 90° rotation on the *x*-axis between each other) of OBP-1F monomer 3D-structure model. Arrow indicates the opening of the putative binding site and the point of view C. Numbers are relative to tyrosine and tryptophan positions in the sequence. Exposed and buried tyrosines are shown in red and blue, respectively. Tyrosine-bound residues through H-bounds (dotted line) are shown in green. Tryptophan 16 is shown in magenta.

its fluorescence spectral properties, although more sensitive, did not significantly change upon ligand binding (data not shown). Thus, the CD spectrum alteration could concern only tyrosyl residues. Tyrosine titration showed that two residues were affected by ligand binding. Y82, which is close to the opening of the cavity and the neighbour Y87, can be likely ruled out from this process. Instead, their OH groups are free and then have a normal pK, revealing no interaction, which remained unchanged upon odorant binding. The

four other tyrosines are more or less buried and involved in H-bonds. One of them could not be titrated even after alkali denaturation, suggesting location in a stable site and/or strong interactions with neighbouring residues. According to the modelled 3D structure, these features could be attributed to Y38, because of its location in a deep crevice and the presence of two H-bonds. In contrast, Y139 appeared more exposed at the surface of the protein and then was likely the residue that has a variable pK between 10 and 11. Then the

Table 2 Possible properties of the tyrosines in OBP-1F according to the modelled 3D structure

Tyrosine	Location	State	H-bond	pK	pK with linalool
20	Strand A	Buried	O-HThr146	11.2	11.7
38	Strand B	Buried	H-NArg36 O-HThr152	–	–
78	Strand E	Buried	H-OCys48	11.2	11.7
82	Strand E	Exposed	None	9.6	9.6
87	Strand F	Exposed	None	9.6	9.6
139	α helix	Intermediate	O-HGlu138	$9.6 < pK < 11.2$	

Bold numbers indicates conserved residues. Dashes indicate undetermined values.

residues whose pK shifted upon ligand binding could be Y20 and Y78. Both these residues are located in two different regions of the protein Y20 on a closed space between the α-helix and the β-barrel, whereas Y78 is covered in a depression by the large loop shaping an opened cavity at the bottom of the protein. The distance between the binding site and the potentially affected residues, which are far from each other, suggests that the alteration of their spectral properties, observed upon ligand binding, originated in a side-chain shift independent of ligand proximity, as could happen for W16. These shifts are then likely to be induced by a local conformational change, which is not limited to the local environment of the reported residues, but a more wide rearrangement of the OBP-1F backbone.

The model of a single binding site per dimer provides the best curve fitting results for binding isotherms measured with any tested ligand and is supported by fluorescence and difference spectroscopy assays. The dimeric state of OBP-1F was confirmed using diffusion light scattering (data not shown). Such a stoichiometry was already reported for several OBP and other lipocalins, whatever the binding test used (Pevsner *et al.*, 1986; Bignetti *et al.*, 1988; Löbel *et al.*, 1998; Burova *et al.*, 1999; Ragona *et al.*, 2000). The OBP binding site would be localized in the hydrophobic cavity shaped by the β-barrel structure, called the calyx (Vincent *et al.*, 2000; Ramoni *et al.*, 2001), as reported for other lipocalins (Flower *et al.*, 2000), even in dimeric β-lactoglobulin in which only one of the two calyces is occupied (Ragona *et al.*, 2000). In dimeric bovine OBP, a third binding site was suggested to be localized at the interface of both monomers (Monaco and Zanotti, 1992) created by swapping of domains (Bianchet *et al.*, 1996; Tegoni *et al.*, 1996). Similar domain swapping cannot occur in rat OBP-1F dimer, because a disulfide bridge between the β-sheet D and the C-terminal domain blocks the α-helix close to the protein core (Briand *et al.*, 2000b). Such a disulfide bridge has been shown to hamper domain swapping (Ramoni *et al.*, 2002). An attempt to follow OBP-1F monomer dissociation through acidification was carried out using diffusion light scattering without success because of the direct transition between the dimer and a reversible aggregation state at pH 3.0 (data not shown). Specifically mutated monomers, unable to associate, would permit elucidation of the question of whether the dimeric state affects ligand binding.

The presented data are consistent with one binding site located in one of the two β-barrels of the OBP-1F dimer. The question arises concerning the determination why only one on the two potential sites was accessible for binding. Among the possible hypotheses, a subtle conformational change correlated with binding of an odorant molecule, which hampers uptake of a second odorant by the other hydrophobic pocket, has been suggested for bovine OBP (Pevsner *et al.*, 1990). Nevertheless, up to now, conformational studies on OBPs have not revealed any detectable change, either in secondary or local structure upon odorant binding (Monaco and Zanotti, 1992), except one concerning the side-chain of the non-conserved Y52 in the monomeric porcine OBP (Vincent *et al.*, 2000). The conformational change observed here could be involved in such a mechanism for the dimeric rat OBP-1F, through a subunit cross-talking in spite of the probable absence of domain swapping. This question needs to be answered by resolution of the 3D structure of OBP-1F in solution and a survey of the spectral shifts induced by ligand binding. Such approaches could be associated with molecular dynamics of the odorant docking on the protein in order clearly to understand the molecular basis of ligand binding onto OBP-1F.

Acknowledgements

References

Bianchet, M.A., Bains, G., Pelosi, P., Pevsner, J., Snyder, S.H., Monaco, H.L. and **Amzel, L.M.** (1996) *The three-dimensional structure of bovine odorant-binding protein and its mechanism of odor recognition.* Nat. Struct. Biol., 3, 934–939.

Bignetti, E., Cavaggioni, A., Pelosi, P., Persaud, K.C., Sorbi, R.T. and **Tirindelli, R.** (1985) *Purification and characterisation of an odorant-binding protein from cow nasal tissue.* Eur. J. Biochem., 149, 227–231.

Bignetti, E., Cattaneo, P., Cavaggioni, A., Damiani, G. and Tirindelli, R. (1988) *The pyrazine-binding protein and olfaction.* Comp. Biochem. Physiol., 90, 1–5.

Bocskei, Z., Groom, C.R., Flower, D.R., Wright, C.E., Phillips, S.E., Cavaggioni, A., Findlay, J.B. and North, A.C. (1992) *Pheromone binding to two rodent urinary proteins revealed by X-ray crystallography.* Nature, 360, 186–188.

Briand, L., Huet, J.C., Perez, V., Lenoir, G., Nespoulous, C., Boucher, Y., Trotier, D. and Pernollet, J.C. (2000a) *Odorant and pheromone binding by aphrodisin, a hamster aphrodisiac protein.* FEBS Lett., 476, 176–185.

Briand, L., Nespoulous, C., Perez, V., Rémy, J.J., Huet, J.C. and Pernollet, J.C. (2000b) *Ligand-binding properties and structural characterization of a novel rat odorant-binding protein variant.* Eur. J. Biochem., 267, 3079–3089.

Briand, L., Nespoulous, C., Huet, J.C., Takahashi, M. and Pernollet, J.C. (2001) *Ligand binding and physico-chemical properties of ASP*2, *a recombinant odorant-binding protein from honeybee (*Apis mellifera *L.).* Eur. J. Biochem., 268, 752–760.

Briand, L., Eloit, C., Nespoulous, C., Bézirard, V., Huet, J.C., Henry, C., Blon, F., Trotier, D. and Pernollet, J.C. (2002) *Evidence of an odorant-binding protein in the human olfactory mucus: location, structural characterization, and odorant-binding properties.* Biochemistry, 41, 7241–7252.

Brooks, B.R., Karplus, M. and Pettit, B.M. (1988) Proteins: A Theoretical Perspective of Dynamics, Structure and Thermodynamics, Advances in Chemistry and Physics, Vol. LXXI. Wiley, New York.

Burova, T.V., Choiset, Y., Jankowski, C.K. and Haertle, T. (1999) *Conformational stability and binding properties of porcine odorant-binding protein.* Biochemistry, 38, 15043–15051.

Burova, T.V., Rabesona, H., Choiset, Y., Jankowski, C.K., Sawyer, L. and Haertlé, T. (2000) *Why has porcine VEG protein unusually high stability and suppressed binding ability?* Biochim. Biophys Acta, 1478, 267–279.

Dal Monte, M., Andreini, I., Revoltella, R. and Pelosi, P. (1991) *Purification and characterization of two odorant-binding proteins from nasal tissue of rabbit and pig.* Comp. Biochem. Physiol., 99B, 445–451.

Dear, T.N., Boehm, T., Keverne, E.B. and Rabbitts, T.H. (1991a) *Novel genes for potential ligand-binding proteins in subregions of the olfactory mucosa.* EMBO J., 10, 2813–2819.

Dear, T.N., Campbell, K. and Rabbitts, T.H. (1991b) *Molecular cloning of putative odorant-binding and odorant-metabolizing proteins.* Biochemistry, 30, 10376–10382.

Felicioli, A., Ganni, M., Garibotti, M. and Pelosi, P. (1993) *Multiple types and forms of odorant-binding proteins in the Old-World porcupine* Hystrix cristata*.* Comp. Biochem. Physiol., 105, 775–784.

Fisher, H.F. and Singh, N. (1995) *Calorimetric methods for interpreting protein-ligand interactions.* Methods Enzymol., 259, 194–221.

Flower, D.R., North, A.C.T. and Sansom, C.E. (2000) *The lipocalin protein family: structural and sequence overview.* Biochim. Biophys. Acta, 1482, 9–24.

Ganni, M., Garibotti, M., Scaloni, A., Pucci, P. and Pelosi, P. (1997) *Microheterogeneity of odorant-binding proteins in the porcupine revealed by N-terminal sequencing and mass spectrometry.* Comp. Biochem. Physiol., 117B, 287–291.

Garibotti, M., Navarrini, A., Pisanelli, A.M. and Pelosi, P. (1997) *Three odorant-binding proteins from rabbit nasal mucosa.* Chem. Senses, 22, 383–390.

Lascombe, M.B., Grégoire, C., Poncet, P., Tavares, G.A., Rosinsky-Chupin, I., Rabillon, J., Goubran-Botross, H., Mazié, J.C., David, B. and Alzari, P.M. (2000) *Crystal structure of the allergen Equ c 1. A dimeric lipocalin within restricted IgE-reactive epitopes.* J. Biol. Chem., 275, 21572–21577.

Laskowski, R.A., McArthur, M.W., Moss, D.S. and Thornton, J. (1993) *PROCHECK: a program to check the quality of protein structures.* J. Appl. Crystallogr., 26, 282–291.

Lazar, J., Greenwood, D.R., Rasmussen, L.E.L. and Prestwich, G.D. (2002) *Molecular and functional characterization of an odorant-binding protein of the Asian elephant,* Elephas maximus: *implications for the role of lipocalins in mammalian olfaction.* Biochemistry, 41, 11786–11794.

Löbel, D., Marchese, S., Krieger, J., Pelosi, P. and Breer, H. (1998) *Subtypes of odorant-binding proteins: heterologous expression and ligand binding.* Eur. J. Biochem., 254, 318–324.

Löbel, D., Strotmann, J., Jacob, M. and Breer, H. (2001) *Identification of a third rat odorant-binding protein (OBP3).* Chem. Senses, 26, 673–680.

Marchese, S., Pes, D., Scaloni, A., Carbone, V. and Pelosi, P. (1998) *Lipocalins of boar salivary glands binding odours and pheromones.* Eur. J. Biochem., 252, 563–568.

Miyawaki, A., Matsushita, F., Ryo, Y. and Mikoshiba, K. (1994) *Possible pheromone-carrier function of two lipocalin proteins in the vomeronasal organ.* EMBO J., 13, 5835–5842.

Monaco, H.L. and Zanotti, G. (1992) *Three-dimensional structure and active site of three hydrophobic molecule-binding proteins with significant amino acid sequence similarity.* Biopolymers, 32, 457–65.

Nespoulous, N. and Pernollet, J.-C. (1994) *Local structural differences between alpha and beta elicitins shown by circular dichroism and ultraviolet difference spectroscopy.* Int. J. and. Protein Res., 43, 154–159.

Ohno, K., Kawasaki, Y., Kubo, T. and Tohyama, M. (1996) *Differential expression of odorant-binding protein genes in rat nasal glands: implications for odorant-binding proteinII as a possible pheromone transporter.* Neuroscience, 71, 355–366.

Oldham, N.J., Krieger, J., Breer, H. and Svatos, A. (2001) *Detection and removal of an artefact fatty acid from the binding site of recombinant* Bombyx mori *pheromone-binding protein.* Chem. Senses, 26, 529–531.

Pace, N.C., Vajdos, F., Fee, L., Grimsley, G. and Gray, T. (1995) *How to measure and predict the molar absorption coefficient of a protein.* Protein Sci., 4, 2411–2423.

Pelosi, P. (1994) *Odorant-binding proteins.* Crit. Rev. Biochem. Mol. Biol., 29, 199–228.

Pelosi, P. (1996) *Perireceptor events in olfaction.* J. Neurobiol., 30, 3–19.

Pelosi, P., Baldaccini, N.E. and Pisanelli, A.M. (1982) *Identification of a specific olfactory receptor for 2-isobutyl-3-methoxypyrazine.* Biochem. J., 201, 245–248.

Pes, D. and Pelosi, P. (1995) *Odorant-binding proteins of the mouse.* Comp. Biochem. Physiol., 112B, 471–479.

Pes, D., Dal Monte, M., Ganni, M. and Pelosi, P. (1992) *Isolation of two odorant-binding proteins from mouse nasal tissue.* Comp. Biochem. Physiol., 103, 1011–1017.

Pes, D., Mameli, M., Andreini, I., Krieger, J., Weber, M., Breer, H. and Pelosi, P. (1998) *Cloning and expression of odorant-binding proteins Ia and Ib from mouse nasal tissue.* Gene, 212, 49–55.

Pevsner, J., Trifiletti, R.R., Strittmatter, S.M. and Snyder, S.H. (1985) *Isolation and characterization of an olfactory receptor protein for odorant pyrazines.* Proc. Natl Acad. Sci. USA, 82, 3050–3054.

Pevsner, J., Sklar, P.B. and Snyder, S.H. (1986) *Odorant-binding protein: localization to nasal glands and secretions.* Proc. Natl Acad. Sci. USA, 83, 4942–4946.

Pevsner, J., Reed, R.R., Feinstein, P.G. and Snyder, S.H. (1988) *Molecular cloning of odorant-binding protein: member of a ligand carrier family.* Science, 241, 336–339.

Pevsner, J., Hou, V., Snowman, A.M. and Snyder, S.H. (1990) *Odorant-binding protein. Characterization of ligand binding.* J. Biol. Chem., 265, 6118–6125.

Ragona, L., Fogolari, F., Zetta, L., Pérez, D.M., Puyol, P., DeKruif, K., Löhr, F., Rüterjans, H. and Molinari, H. (2000) *Bovine β-lactoglobulin: interaction studies with palmitic acid.* Protein Sci., 9, 1347–1356.

Ramoni, R., Vincent, F., Grolli, S., Conti, V., Malosse, C., Boyer, F.D., Nagnan-le Meillour, P., Spinelli, S., Cambillau, C. and Tegoni, M. (2001) *The insect attractant 1-octen-3-ol is the natural ligand of bovine odorant-binding protein.* J. Biol. Chem., 276, 7150–7155.

Ramoni, R., Vincent, F., Ashcroft, A.E., Accornero, P., Grolli, S., Valencia, C., Tegoni, M. and Cambillau, C. (2002) *Control of domain swapping in bovine odorant-binding protein.* Biochem. J., 365, 739–748.

Rouvinen, J., Rautiainen, J., Virtanen, T., Zeiler, T., Kauppinen, J., Taivainen, A. and Mäntyjärvi, R. (1999) *Probing the molecular basis of allergy. 3-dimensional structure of the bovine lipocalin allergen Bos d 2.* J. Biol. Chem., 274, 2337–2343.

Sali, A. and Blundell, T.L. (1993) *Comparative protein modelling by satisfaction of spatial restraints.* J. Mol. Biol., 234, 779–815.

Scaloni, A., Paolini, S., Brandazza, A., Fantacci, M., Bottiglieri, C., Marchese, S., Navarrini, A., Fini, C., Ferrara, L. and Pelosi, P. (2001) *Purification, cloning and characterization of odorant- and pheromone-binding proteins from pig nasal epithelium.* Cell. Mol. Life Sci., 58, 823–834.

Spinelli, S., Ramoni, R., Grolli, S., Bonicel, J., Cambillau, C. and Tegoni, M. (1998) *The structure of the monomeric porcine odorant-binding protein sheds light on the domain swapping mechanism.* Biochemistry, 37, 7913–7918.

Spinelli, S., Vincent, F., Pelosi, P., Tegoni, M. and Cambillau, C. (2002) *Boar salivary lipocalin: 3-dimensional X-ray structure and androstenol/androstenone docking simulations.* Eur. J. Biochem., 269, 2449–2456.

Steinbrecht, R.A. (1998) *Odorant-binding proteins: expression and function.* Ann. N. Y. Acad. Sci., 855, 323–332.

Tachibana, A. and Murachi, T. (1966) *Phenolic hydroxyl ionization in stem bromelain.* Biochemistry, 5, 2756–2763.

Tegoni, M., Ramoni, R., Bignetti, E., Spinelli, S. and Cambillau, C. (1996) *Domain swapping creates a third putative combining site in bovine binding protein dimer.* Nat. Struct. Biol., 3, 863–867.

Tegoni, M., Pelosi, P., Vincent, F., Spinelli, S., Campanacci, V., Grolli, S., Ramoni, R. and Cambillau, C. (2000) *Mammalian odorant-binding proteins.* Biochim. Biophys Acta, 1482, 229–240.

Utsumi, M., Ohno, K., Kawasaki, Y., Tamura, M., Kubo, T. and Tohyama, M. (1999) *Expression of major urinary protein genes in the nasal glands associated with general olfaction.* J. Neurobiol., 39, 227–236.

Vincent, F., Spinelli, S., Ramoni, R., Grolli, S., Pelosi, P., Cambillau, C. and Tegoni, M. (2000) *Complexes of porcine odorant-binding protein with odorant molecules belonging to different chemical classes.* J. Mol. Biol., 300, 127–139.

Vincent, F., Löbel, D., Brown, K., Spinelli, S., Grote, P., Breer, H., Cambillau, C. and Tegoni, M. (2001) *Crystal structure of aphrodisin, a sex pheromone from female hamster.* J. Mol. Biol., 305, 459–469.